

Modelling and control of Automatic Guided Vehicles (AGVs) for the transport of meals, laundry and waste in the healthcare domain

Dr.-Ing. Johannes Fottner¹, T. Kerscher², G. di Gropello³, A. Stella³

¹ Swisslog TELELIFT GmbH, Puchheim, Germany, e-mail: Johannes.fottner@swisslog.com

² Universität Karlsruhe, ITEC Prof. Dillmann, c/o Technologiefabrik, Haid-und-Neu-Str. 7, 76137 Karlsruhe, Germany, kerscher@fzi.de.

³ EICAS Automazione S.p.A., Italy, gmg@eicas.it, stella@eicas.it

Abstract

Swisslog TELELIFT developed an AGV that navigates only by the use of odometric data, the sensor data of two 2d-laser-scanners and different specific strategies. Compared with other typically cabled guided AGVs this has the big advantage that no structural changes on a building are necessary. Due to the industrial use, there are many requirements for the AGV concerning security, robustness, precision and operability of the systems. In this paper a kinematic and dynamic model for the AGV of TELELIFT is introduced. The actual used control is presented and the control developed with the help of the EICASLAB using the methodologies proposed during the ACODUASIS project is presented.

Keywords: AGV, modelling, automatic control, mobile robotic

1 Introduction

Swisslog TELELIFT developed an AGV that navigates only by the use of odometric data, the sensor data of two 2d-laser-scanners and different specific strategies. Compared with other typically cabled guided AGVs this has the big advantage that no structural changes on a building are necessary. Due to the industrial use, there are many requirements for the AGV concerning security, robustness, precision and operability of the systems.

The transportation task of the AGV requires for example the recognition and identification of containers that should be transported. The containers are picked up automatically and are transported to different support areas depending on the goods that are loaded. The AGV should drive on predefined logical paths that are represented in a graph with edges and nodes. The AGV should drive strictly on the predefined curves. The drive control must always hold the AGV on this predefined curve. For the control of steering and forward motion PID Controllers are used that were set experimentally. With the help of a new dynamic model for the AGV controllers are developed in EICASLab [1]. These controllers are tested in the simulation environment of EICASLab and directly on the AGV [2]. With the help of this controllers the drive behaviour of the AGV should be improved

Due to the industrial use, there are many requirements for the AGV concerning security, robustness, precision and operability of the systems.



Fig. 1. (left)AGV of Telelift (right) AGV in hospital tunnel

2 Technical description of the AGV

The AGV should drive on predefined logical paths. Edges and nodes (kinks) define these paths; figure 2 shows such a graph. The localisation of the AGV is done with the help of two encoder wheels and two angular sensors on the drive wheels (see figure 3). By continuous matching of the laser scanner data with a predefined map of the environment, the errors of the encoders are corrected. The AGV should drive strictly on the predefined curves. The drive control must always hold the AGV on this predefined curve.

If there is a kink in the target curve, the AGV should drive on an optimal circular arc between the two linear curve segments (figure 2 bottom). This optimal circular arc is defined through the desired speed of the AGV and the angle between the two linear curve segments.

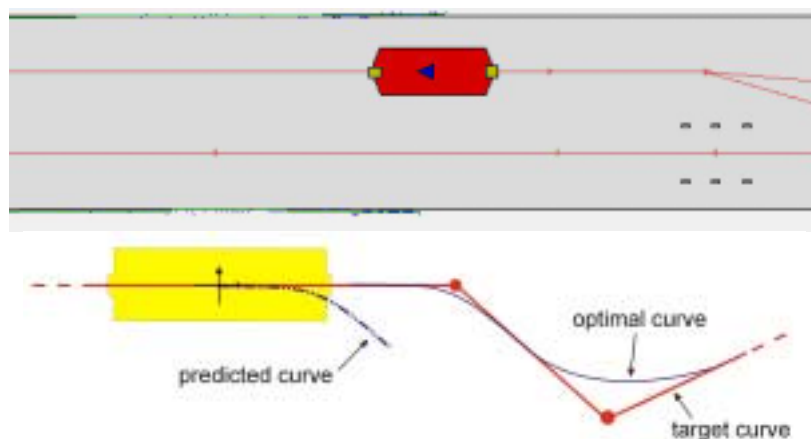


Fig. 2. (top) Navigation path of one AGV (bottom) Predefined curve and optimal curve

2.1 Technical build-up of the AGV

The AGV has a length of 1656 mm and a width of 650 mm. It has two drive wheels, which are necessary for steering and for the motion. They are located at the longitudinal axis of the AGV. The midpoint of the axis connecting the two drive wheels is displaced by 34,1mm from the middle of the robot. The two encoder wheels are located at this point, displaced by 266.5 mm

out of the longitudinal axis. The arrangement of the different wheels is shown in. The AGV has a height of 350 mm without container.

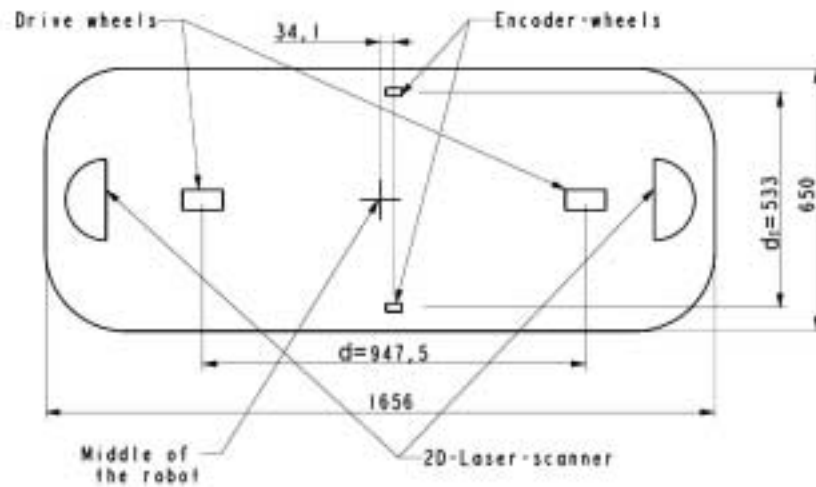


Fig. 3. Schematic build-up of the AGV [mm]

Only one of the drive wheels is powered. It has one motor for driving the AGV forward and backward, and one motor for steering. The other drive wheel is passive and is directly connected to the active one by a steering rod. Because of this, the AGV drives always on a circle (see figure 4).

All this parameters are for the AGV without payload. The AGV has a weight of about 200 kg and it is able to carry containers with the weight up to 400 kg. The dimensions of the AGV are of course different in the case of transporting a container. Especially the centre of gravity varies in this case.

In the current configuration, the AGV has a maximum speed of 1.2 m/s. In the case of an emergency stop, it has a maximum braking distance of about 0.2 m. The maximum steering angle is 47° .

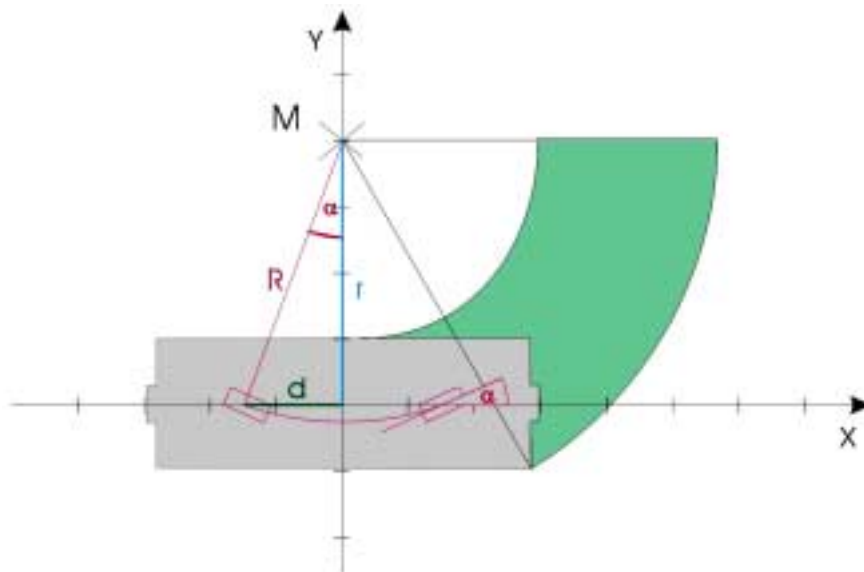


Fig. 4. Drive behaviour of the TELELIFT AGV

3 Model of the AGV

3.1 Kinematic Model of the AGV

It is assumed that the AGV drives on a horizontal plan. Therefore, from the kinematical view it is only a 2D problem. The vehicle has two degree of freedom: the forward motion and the rotation about the z-axis. The motion is influenced of the two motors one for the angle α and the other for the speed of the driving wheels. The AGV drives always on a circle. The radius r (centre of AGV) and R (circle of the driving wheels) depend on the angle α (see figure 4):

$$r = \frac{d}{2 \cdot \tan(\alpha)}, \quad R = \frac{d}{2 \cdot \sin(\alpha)} \quad (1).$$

For a simple kinematical description of the AGV the following differential equation describes the behaviour of the agv:

$$\begin{aligned} \dot{x}_{DW} &= v_{DW} \cdot \cos(\tau - \alpha), & \dot{y}_{DW} &= v_{DW} \cdot \sin(\tau - \alpha) \\ \dot{\tau} &= 2 \cdot \frac{v_{DW}}{d} \cdot \sin(\alpha) \end{aligned} \quad (2)$$

With τ the orientation angle of the AGV to the x-axis, v_{DW} the speed of the drive wheel, α the steering angle of the drive wheel and d distance between the steering wheels. The position of the AGV-middle can be calculated as follows:

$$x_{AGV} = x_{DW} + \frac{d}{2} \cdot \cos(\tau), \quad y_{AGV} = y_{DW} + \frac{d}{2} \cdot \sin(\tau) \quad (3)$$

The speed of the AGV can be calculated by:

$$v_{AGV} = v_{DW} \cdot \cos(\alpha). \quad (4)$$

The position and the speed of the two encoder wheels (left wheel: v_{EL} , right wheel: v_{ER}) are:

$$\begin{aligned} x_{EL} &= x_{DW} + \frac{d}{2} \cdot \cos(\tau) - \frac{d_E}{2} \cdot \sin(\tau), & x_{ER} &= x_{DW} - \frac{d}{2} \cdot \cos(\tau) + \frac{d_E}{2} \cdot \sin(\tau) \\ y_{EL} &= y_{DW} + \frac{d}{2} \cdot \sin(\tau) + \frac{d_E}{2} \cdot \cos(\tau), & y_{ER} &= y_{DW} - \frac{d}{2} \cdot \sin(\tau) - \frac{d_E}{2} \cdot \cos(\tau). \\ v_{EL} &= v_{AGV} \cdot \left(1 - \frac{d_E}{d} \cdot \tan(\alpha)\right), & v_{ER} &= v_{AGV} \cdot \left(1 + \frac{d_E}{d} \cdot \tan(\alpha)\right) \end{aligned} \quad (5)$$

d_E is the distance between the encoder wheels. The position and speed of the front drive-wheel is:

$$\begin{aligned} x_{DWF} &= x_{DW} + d \cdot \cos(\tau), & y_{DWF} &= y_{DW} + d \cdot \sin(\tau) \\ v_{DWF} &= v_{AGV} \cdot \frac{1}{\cos(\alpha)}. \end{aligned} \quad (6)$$

3.2 Dynamic Model of the AGV

For the dynamic model all forces and torques are used to describe the behaviour of the AGV (see figure 5).

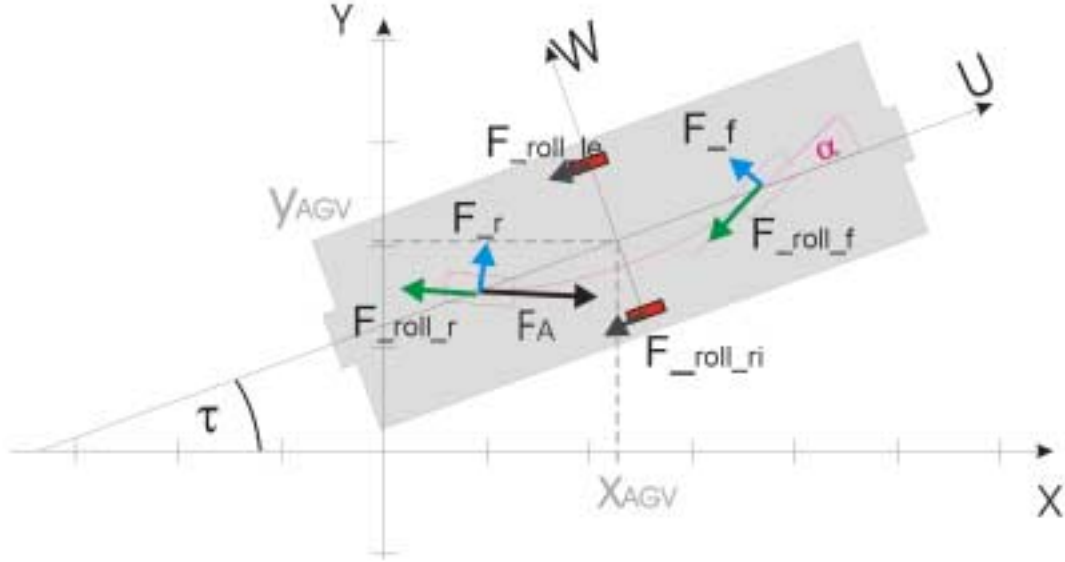


Fig. 5. Forces and torques which interacts with the AGV

Normally the AGV drives only on a horizontal plain, so in the direction of the z-axis there is force equilibrium and it is assumed that there is no resulting torque around the x- and y-axis. So the Forces in z-direction for each wheel can be calculated:

$$m_{AGV} \cdot \ddot{z} = 0 = \sum F_z = F_{EL-Z} + F_{ER-Z} + F_{DWF-Z} + F_{DWR-Z} - F_G \quad (7)$$

with $F_{EL-Z} = F_G \cdot \frac{d}{2 \cdot (d_E + d)}$, $F_{ER-Z} = F_G \cdot \frac{d}{2 \cdot (d_E + d)}$, $F_{DWF-Z} = F_G \cdot \frac{d_E}{2 \cdot (d_E + d)}$ and

$$F_{DWR-Z} = F_G \cdot \frac{d_E}{2 \cdot (d_E + d)}.$$

With the help of these forces the rolling friction forces of the wheels can be calculated. The roll-

ing frictions of the wheels are $F_{roll_{(f/r)}} = \frac{\mu_{roll}}{r_{DW}} \cdot F_{DW(F/R)-Z}$, $F_{roll_{(le/ri)}} = \frac{\mu_{roll}}{r_{EW}} \cdot F_{EW(L/R)-Z}$ with

μ_{roll} the rolling friction coefficient and r_{DW} , r_{EW} the radius of the two wheels. The effective direction of the rolling friction is always against the roll direction of the wheel. The side forces of the driving wheels are:

$$F_{(f/r)} = K_{(f/r)} \cdot \beta_{(f/r)} \quad (8)$$

with $K_{(f/r)}$ the concerning stiffness of the wheels and the slip angle $\beta_{(f/r)}$. This angle can be calculated as follows:

$$\beta_f = \alpha - \frac{v_w + \frac{d}{2} \cdot \omega}{v_U}, \quad \beta_r = \alpha + \frac{v_w - \frac{d}{2} \cdot \omega}{v_U} \quad (9)$$

With the help of these forces, the equation of motion can be formulated as follows:

$$\begin{aligned} m_{AGV} \cdot (\ddot{u} - v_w \cdot \omega) &= \sum F_U = F_{A-U} - F_{roll_f-U} - F_{roll_r-U} - F_{roll_le-U} - F_{roll_le} - F_{roll_ri} + F_{r-U} - F_{f-U} \\ m_{AGV} \cdot (\ddot{w} + v_U \cdot \omega) &= \sum F_W = -F_{A-W} - F_{roll_f-W} + F_{roll_r-W} + F_{r-W} + F_{f-W} \\ I_{zAGV} \cdot \ddot{\tau} &= \sum M_z = F_A \cdot l_1 - F_f \cdot l_2 + F_r \cdot l_2 - F_{roll_r} \cdot l_1 - F_{roll_f} \cdot l_1 - F_{roll_ri} \cdot \frac{d_E}{2} + F_{roll_le} \cdot \frac{d_E}{2} \end{aligned} \quad (10)$$

with

$$\begin{aligned} F_{A-U} &= F_A \cdot \cos(\alpha), & F_{A-W} &= F_A \cdot \sin(\alpha), & F_{roll_f-U} &= F_{roll_f} \cdot \cos(\alpha), \\ F_{roll_f-W} &= F_{roll_f} \cdot \sin(\alpha), & F_{roll_r-U} &= F_{roll_r} \cdot \cos(\alpha), & F_{roll_r-W} &= F_{roll_r} \cdot \sin(\alpha), \\ F_{roll_re-U} &= F_{roll_re} \cdot \cos(\alpha), & F_{roll_re-W} &= F_{roll_re} \cdot \sin(\alpha), & F_{roll_li-U} &= F_{roll_li} \cdot \cos(\alpha), \\ F_{roll_li-W} &= F_{roll_li} \cdot \sin(\alpha), & F_{r-U} &= F_r \cdot \sin(\alpha), & F_{r-W} &= F_r \cdot \cos(\alpha), & F_{f-U} &= F_f \cdot \sin(\alpha), \\ F_{f-W} &= F_f \cdot \cos(\alpha) \text{ and } l_1 = \frac{d}{2} \cdot \sin(\alpha), & l_2 &= \frac{d}{2} \cdot \cos(\alpha). \end{aligned}$$

The driving wheel with the help of an electric motor produce the force F_A , which can be calculate with the help of the torque of the e-motor M_{EM} :

$$F_A = \frac{M_{EM}}{r_{DW} \cdot n_{gear} \cdot \eta_{gear}} \quad (11)$$

with the ratio of the gear n_{gear} and the efficiency of the gear η_{gear} . The rotating speed of the drive wheel can be calculated based on the speed of the agv in the U-direction:

$$\omega_{DW} = \frac{v_U}{r_{DW} \cdot \cos(\alpha)}. \quad (12)$$

The torque of the e-motor M_{EM} is calculated by the help of the robotic toolbox.

4 Control of the AGV

4.1 Control algorithm implemented on the real AGV

The steering-controller works only with the help of the actual position, the orientation α and the actual speed v of the AGV.

The AGV is localized with the help of two coordinates and the orientation. The control does not work with target points (for example the nodes). It tries to hold the AGV on the edges of the predefined graph. For this, it is necessary to know the last and the two next nodes. Therefore, the target curve is well defined.

The first target of the steering-controller is to drive the AGV on the predefined curve. In order to keep this goal, the controller has to minimize the lateral offset Δ_l and the orientation error Δ_α (see figure 6). The output of the controller (target steering angle α_s) is calculated with the following equation:

$$\alpha_s = \frac{d_\alpha \cdot \Delta_\alpha + d_l \cdot \Delta_l}{d_v \cdot (v + v_{\min})} \quad (13)$$

There are different parameters, which are set manually: angle parameter d_α , distance parameter d_l , velocity parameter d_v and minimum velocity v_{\min} . The target steering angle is set by an external PID-controller, executed on a micro controller.

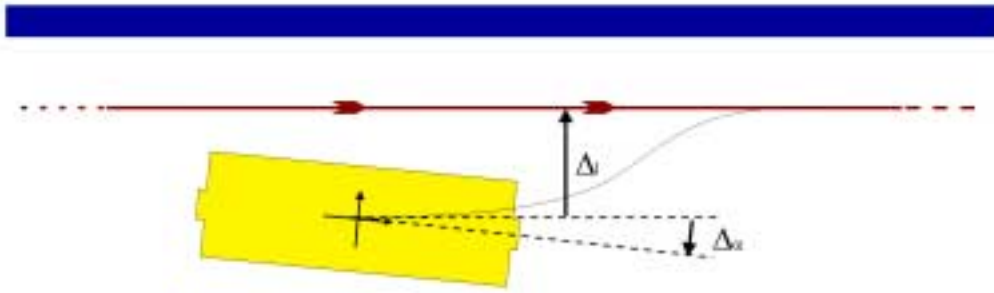


Fig. 6. Position and orientation error for the easy control strategy of TELELIFT

The second task for the controller is to hold the AGV on the optimal circular curve in case of kinks and for big disturbance. The AGV can only drive circularly, so there must be an approximation for the driving lane. In figure 7 the optimal curve for a target curve is shown. The optimal curve depends on the angle between the two linear edges belonging to the node (kink) and the desired drive-speed. Nevertheless, it is also influenced by the following course of the target curve.

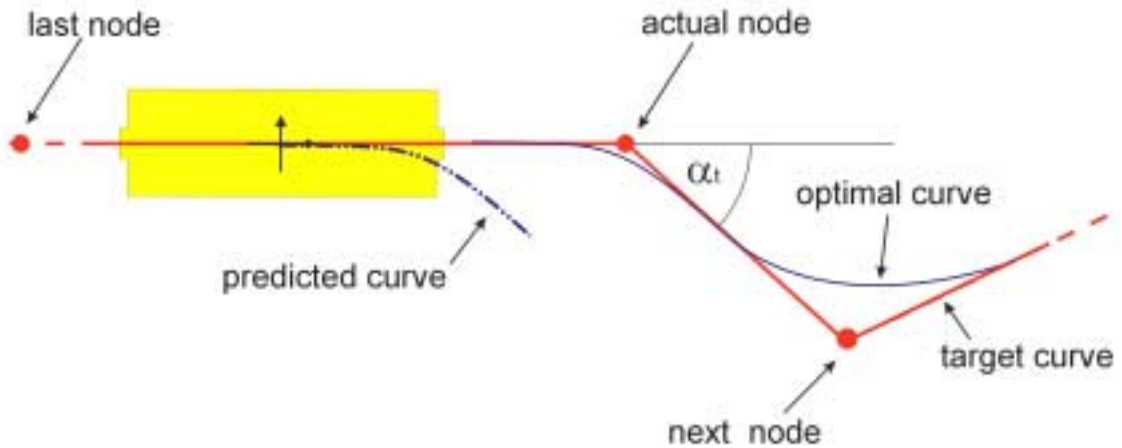


Fig. 7. Predefined curve and optimal curve with respect to the AGV kinematics

Currently an algorithm is used which calculates the optimal curve for the next kink on basis of the actual and the next node. Every iteration step the controller checks if this predicted curve in-

tersects the next edge of the target curve. If an intersection took place, the controller starts to use the optimal curve as desired curve until the driving lane of the AGV is congruent with the next edge of the target curve.

The predicted curve is calculated with an initial steering angle α_{Steer} to receive the optimal circular path for the actual to the next path of the driving graph. The position to start the steering depends on the angle between actual and next path and from the desired steering angle.

The steering process starts if the end position for the steering intersects the next path of the driving graph. During the steering process it is checked every iteration if the end point lies on the predefined curve. If this is not the case the steering angle is modified by a bang-bang controller (end point to near then $\alpha_{Steer,i} = \alpha_{Steer,i-1} \cdot 0.9$; end point to far then $\alpha_{Steer,i} = \alpha_{Steer,i-1} \cdot 1.1$).

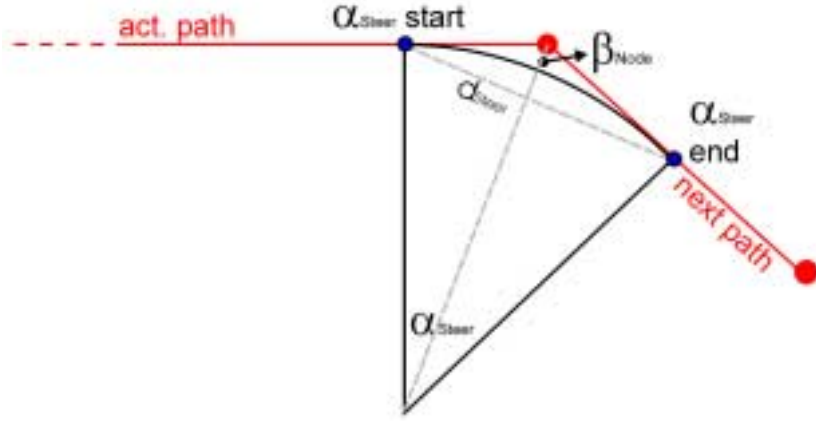


Fig. 8. Calculation of start and end position to steer

It is assumed, that the controller can set the steering angle in zero time. The initial steering angle is set to $\alpha_{Steer} = 36 \text{ GRAD}$.

The second part of the steering control is activated if there is an angle difference bigger than 5 degree. Otherwise, the first part of the controller is able to drive the vehicle accurate on the predicted path.

4.2 Control algorithm realized with the help of the EICASLAB software tool

Simplified model

According to the EICAS approach for the control system design a simplified model, that describes the plant within the frequency band of interest, has been considered.

It has been considered to command directly the steering angle α , considering to have a low-level control fast enough for actuating the requested α .

It was then possible, for the simplified model definition, to consider the kinematic equations: setting:

x, y	the coordinates of the barycentre of the AGV,
τ	the orientation angle of the AGV to the x-axis,
v	the speed of the AGV,
d	is the distance between the two drive wheels,

it is possible, according to par.3.1, to write:

$$\begin{cases} \dot{x} = v \cdot \cos \tau \\ \dot{y} = v \cdot \sin \tau \\ \dot{\tau} = \frac{2v}{d} \cdot \tan \alpha \end{cases}$$

The aim, expect during the curves, is to follow a straight line: then, starting from the command α we want to control the orientation angle of the AGV, τ , and the distance between a straight line and the AGV which will be denoted by D . By using an appropriate reference generator which increases the desired τ and D during the curves, it is possible to use always the same simplified model.

For the simplified model, considering that α is never greater than 40° it is assumed $\tan \alpha \approx \alpha$, and then

$$\tau(i+1) = \tau(i) + Ts \cdot \frac{2v}{d} \cdot \alpha$$

(where Ts is the sampling time).

The distance between the straight line and the AGV is constant if the orientation of the AGV is equal to the one of the straight line, in all cases it is:

$$D(i+1) \cong D(i) + Ts \cdot v \cdot \sin(\tau - \tau_{straightline}) \cong D(i) + Ts \cdot v \cdot (\tau - \tau_{straightline})$$

The simplified model is shown in figure 9.

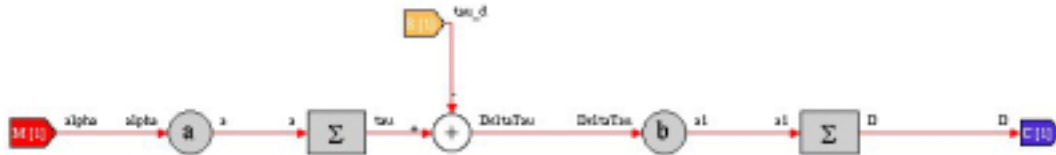


Fig.9. Simplified model

$$a = 2 \cdot v \cdot Ts / d$$

$$b = v \cdot Ts$$

τ is the orientation of the AGV ,

τ_d is the desired orientation of the AGV ,

D is the distance between the AGV and the straight line that it is following.

Control structure

The control, according to EICAS methodology is composed by a reference generator, an observer and a control.

The control structure is depicted in the following figure:

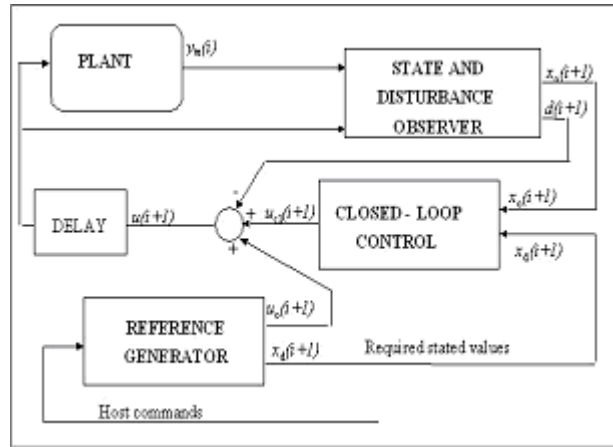


Fig.10. Observer

Reference generator

Except during the curves the AGV must follow a straight line: in that case the open loop command (indicated by 'u_o' in fig.10) is $\alpha_o=0$ and the desired τ and D are :

$$\begin{aligned} \tau_d &= \tau_{straight\ line} \\ D_d &= 0 \end{aligned}$$

The global path has been provided by means of the coordinates of the nodes; for the curves the reference generator generates a trajectory considering an 'optimal' curve.

The trajectory is computed considering three parameters: the maximum acceleration, the maximum speed, and the maximum value, of $\alpha(t)$: the acceleration is always set equal to its maximum or to zero.

The reference generator computes the distance from the actual node at which the curve must begin: when the AGV reaches this distance it begins to curve: it must move away from its current straight line (the line joining the last node with the actual one) and reach the next one (the line joining the actual node with the next one): the trajectory is provided by means of the open loop command (α_o) and the desired orientation (τ_d) and distance (D_d), computed for every step.

τ_d changes, in a continuous way, from $\tau_{current\ straight\ line}$ to $\tau_{next\ straight\ line}$;

D_d increases at the beginning of the curve since the AGV must move away from the current straight line, and when the AGV reaches the half of its trajectory (the bisecting line of the current straight line and the next one) it decreases.

Observer

The observer structure is shown in figure 11.

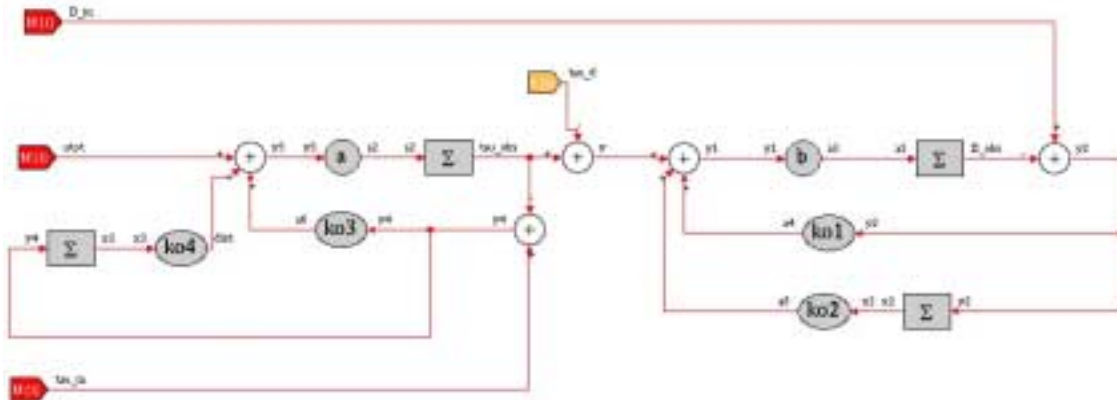


Fig.11. Observer

Control

The control structure is shown in figure 12.

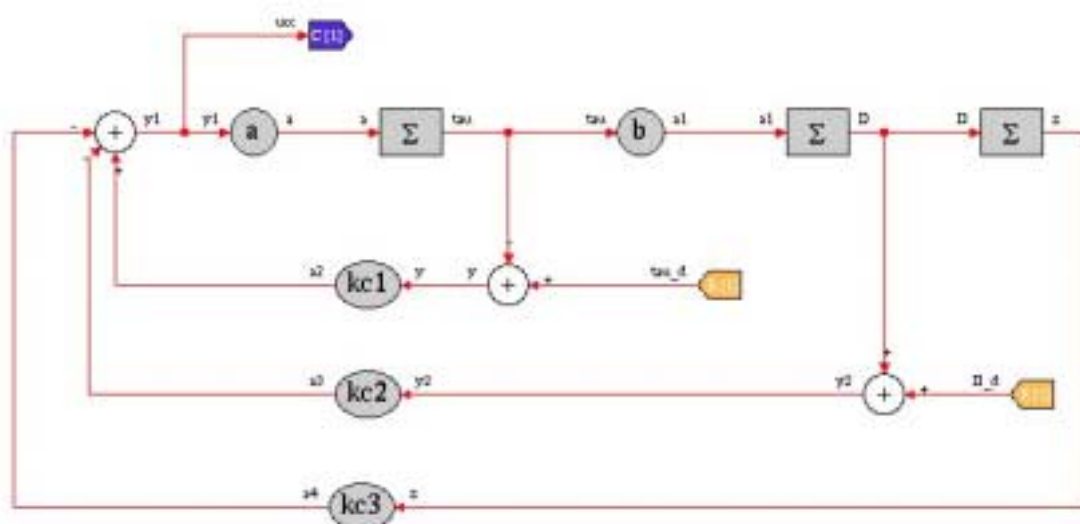


Fig.12. Control

Simulation results

As test the path shown in the Fig.13 has been considered.

Starting from an initial orientation ($\tau_{init} = 0.1 \text{ rad}$) the AGV must go on the desired trajectory and follow it.

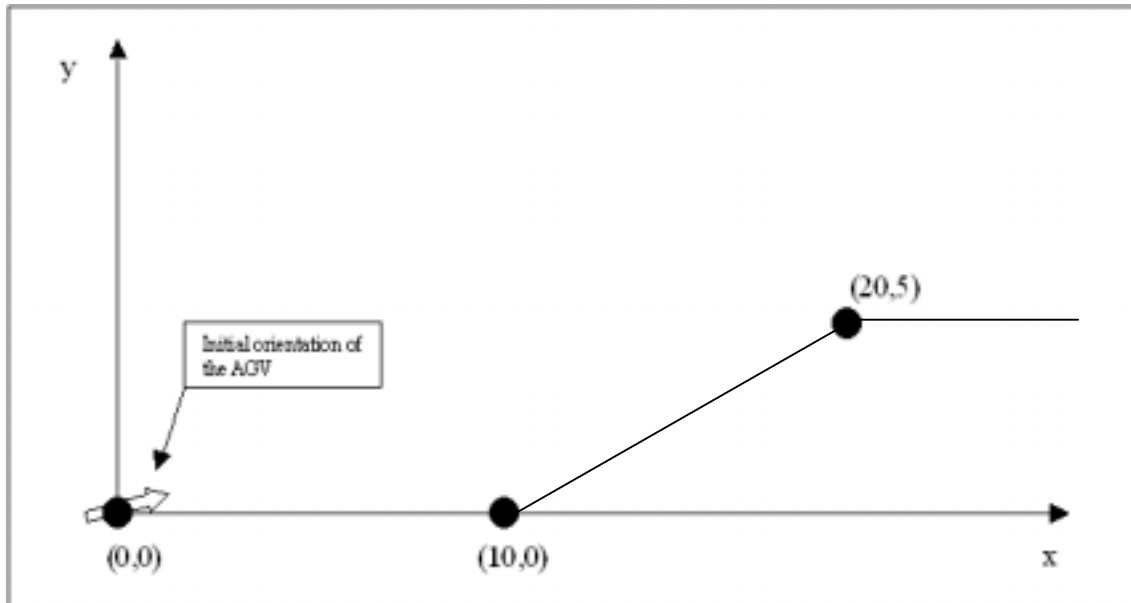


Fig. 13. Desired path

The next figure shows the path followed, during the simulation, by the AGV (the red lines are the lines joining the nodes, the black line is the path of the AGV):



Fig.14. AGV Trajectory

the orientation of the AGV has an initial value of 0.1 rad , it must follow a straight line with $\tau=0 \text{ rad}$, then a straight line with $\tau=0.464 \text{ rad}$, and finally a straight line with $\tau=0 \text{ rad}$. The next figure shows the orientation:

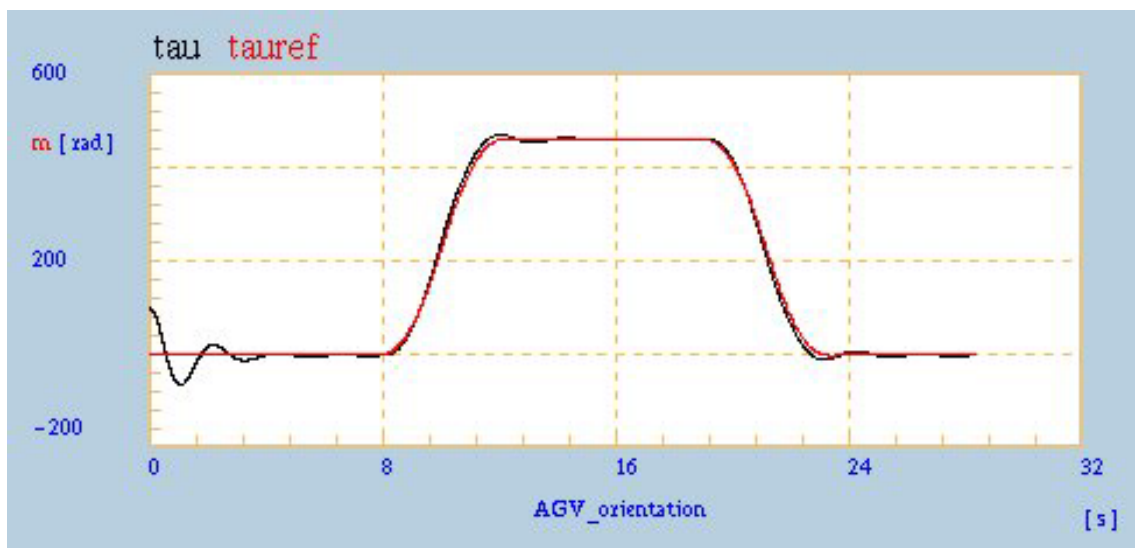


Fig.15. AGV orientation

the next figure shows the reference distance, which increases at the beginning because of the initial bad orientation, and then increases and decreases during the curves:



Fig.16. AGV distance from the reference straight lines

Finally, the following figure shows the command α :

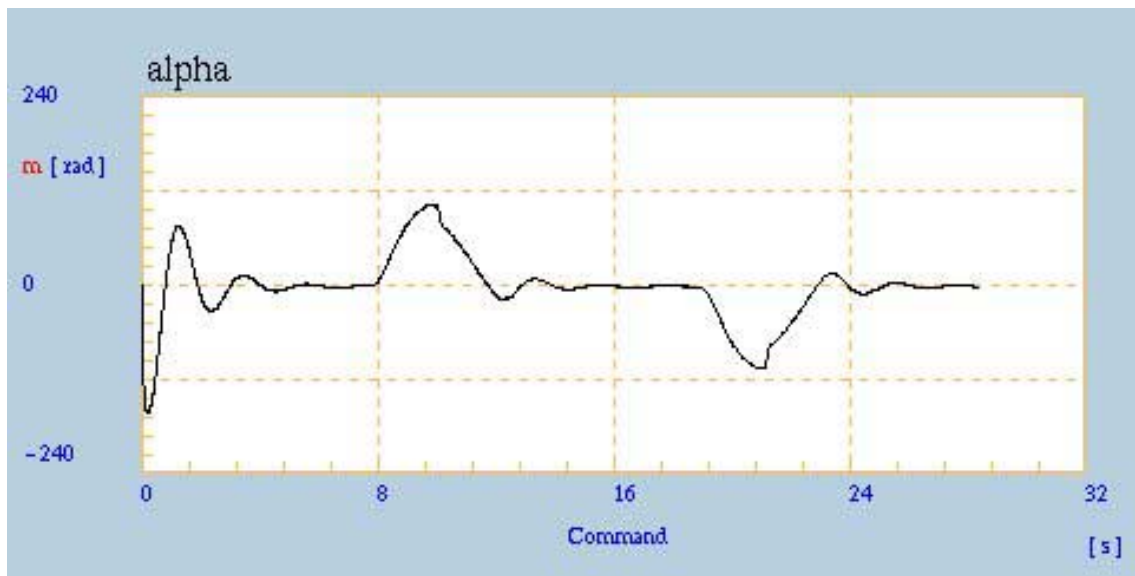


Fig.17. Command

5. Conclusion and Outlook

The control of the AGV was implemented in a very un scientific way, but the results fits the requirements for the AGV. With the help of the advance simulation software EICASLAB a new control design is presented which fits also the requirements. The result of both controls shown that the control developed using the methodology proposed in the ACODUASIS project is more sophisticated. Especially the use of the dynamics for the control design is necessary to receive better results in the driving behaviour. So the mechanics are not so stressed and the lifetime of the AGV is increased.

Acknowledgements

The work has been realised within the ACODUASIS Project [3] (IPS-2001-42068), a three-year project founded by the European Commission in the frame of the Innovation Program.

References

1. G. Caporaletti, *The ACODUASIS project – a professional software tool supporting the control design in robotics*, In Proc. of the 6th International Conference on Climbing and Walking Robots (CLAWAR), 2003.
2. F. Donati, M. Vallauri: *Guaranteed control of almost- linear plants*. IEEE Transactions on Automatic Control, vol. 29- AC, 1984, pp. 34-41.
3. Website of the ACODUASIS-project funded by the European Community: <http://www.fzi.de/acoduasis>, September 2005.